Communications in Physics, Vol. 32, No. 1 (2022), pp. 1-9
DOI: https://doi.org/10.15625/0868-3166/16091

CHARACTERISTICS OF DYE-DOPED SILICA NANOPARTICLES- BASED RANDOM LASERS IN THE AIR AND WATER

TA VAN DUONG[1,†], NGUYEN TRONG TAM[2], MAI HONG HANH[2], NGUYEN XUAN THAU[3] AND NGHIEM THI HA LIEN[4]

[1]*Department of Optical Devices, Le Quy Don Technical University, Hanoi 100000, Vietnam*

[2]*Department of Quantum Optics, Faculty of Physics, University of Science, Vietnam National University, Hanoi 100000, Vietnam*

[3]*Department of Physics, Le Quy Don Technical University, Hanoi 100000, Vietnam*

[4]*Institute of Physics, Vietnam Academy of Science and Technology, Hanoi 100000, Vietnam*

E-mail: †duong.ta@lqdtu.edu.vn

Received 26 May 2021; *Accepted for publication 24 September 2021*; *Published 15 January 2022*

Abstract. *Random lasers based on dye-doped silica nanoparticles are attracted for biomedical applications due to their biocompatibility and high brightness. Several laser structures including silica powder and film have been reported. However, the dependence of lasing characteristics including lasing threshold and emission wavelength on the laser size and working environment have not been explored. Here, we demonstrate and compare the lasing characteristics of dye-doped silica random lasers in the air and water. These lasers present in thin structures, the so-called microslices, with a thickness of 1 μm and various dimensions from 30 to 300 μm. It is found that the lasing threshold (I_{th}) decreases with increasing laser size such as $I_{th} \sim A^{-0.66}$ for sample in the air and $I_{th} \sim A^{-0.45}$ for sample in the water, where A is the sample surface area. For a similar size, the lasing threshold of the sample in the water is about 3-8 times higher than that of the sample in the air. In addition, the lasing peak wavelength exhibits a red-shift with increasing the laser size. In the air, a shift of 8 nm is recorded when the sample surface area increases from* 21×10^3 *to* 169×10^3 μm^2. *Furthermore, for a similar size, the lasing wavelength of the sample in the air is also red-shifted (13 nm on average) compared with that of the sample in the water. Our finding provides useful information for the use of silica-based random lasers in bioimaging and biosensing applications.*

Keywords: random laser, microlaser, dye-doped silica nanoparticles, film.

Classification numbers: 42.55.Tv; 82.35.Np.

I. INTRODUCTION

Recently, random lasers have drawn a great deal of attention due to their special optical properties [1] and wide range of photonic applications [2–4]. Especially, random lasers utilizing biocompatible materials have shown promising prospects for bio-imaging and biosensing [5–7]. Unlike the conventional lasers that rely on the resonant circulation of light in an optical cavity [8, 9], random lasers do not have a cavity, their emission is amplified by multiple scatters of light in an active medium. As a result, compared with conventional lasers, random lasers have several advantages such as simpler fabrications and better emission stability (less affected by cavity defects). Indeed, random lasers can be achieved from various disordered structures including dye-doped metallic nanoparticles powder [3], clusters [10–12], and biological tissues/structures [13–16].

Among many biocompatible materials, dye-doped silica nanoparticles (SNPs) are an excellent gain material due to their high photoluminescence (PL) intensity and photostability [17]. Indeed, random lasers have been realized from dye-doped silica gel powder [18, 19]. Recently, random lasers have been obtained from dye-doped SNP film structures [20]. However, none of those work has studied the effect of laser size and working environment on lasing characteristics including lasing threshold and wavelengths.

In this work, we demonstrate random lasing from dye-doped SNP film-like structures and compare their lasing characteristics for different sizes in the air and in the water. Our study provides important information for future applications of random lasers in biosensing and bioimaging.

II. EXPERIMENT

II.1. Fabrication of dye-doped silica film structure

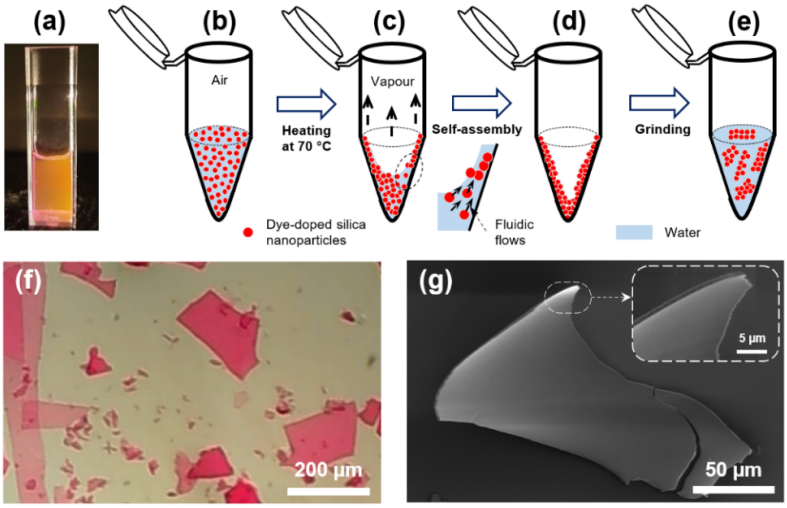

Fig. 1. (a) RhB-doped SNP solution illuminated by a halogen lamp. (b)-(e) Process in which SNPs are self-assembled to a film structure. (f) Optical microscope image of RhB-doped SNP microslides. (g) SEM image of a typical SNP microslide.

The random laser was based on a silica nanoparticle film which was self-assembled from a Rhodamine B (RhB)-doped SNP solution (Fig. 1a). These SNPs were synthesized by a modified Stober method and have a size of around 20 nm [17]. Firstly, a 200 μL of the dye-doped SNP solution was injected into an Eppendorf tube (Fig. 1b) and subsequently heated at a stable temperature of 70˚C (in an oven) for 3 hours. Due to the high temperature, water gradually evaporates which induces fluidic flow [21] and subsequently drives SNPs toward the pinning of the contact line at the tube wall (Fig. 1c). In the end, a film of nanoparticles is formed (Fig. 1d). For optical characterization, the film was ground into multiple pieces, the so-called microslices (Fig. 1e) with dimensions ranging from around 20 to 300 μm (Fig. 1f). SEM image of a typical dye-doped SNP piece is shown in Fig. 1g indicating a microslice with a smooth surface and thickness of about 1 μm.

II.2. Optical characterization

The optical properties of RhB-doped SNP microslice in the air and in the water were characterized by utilizing a micro-photoluminescence (μ-PL) setup as demonstrated in Fig. 2 [22]. The pumping source is Nd:YAG nanosecond (ns) pulse Q-switch laser (Litron laser) with a wavelength of 532 nm, a repetition rate of 10 Hz and a pulse duration of 7 ns. The excitation beam was focused on a spot of 350 μm in diameter. The emission from the sample was collected via a 10X objective lens and delivered to a spectrometer (Avantes AvaSpec-2048L) for spectral recording. The spectral resolution is $\sim$0.2 nm. In addition, for the size-dependent characterization, the surface area of the sample was determined from optical microscope images by using ImageJ software.

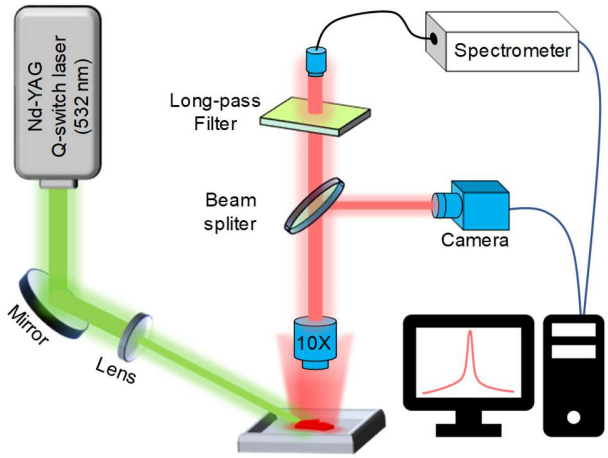

Fig. 2. Schematic of a μ-PL setup used for optical characterization.

III. RESULTS AND DISCUSSIONS

III.1. Random lasing in the air and water

Figure 3a plots the PL spectra of a microslice (dimension of 150$\times$120 μm) under increasing pump pulse energy (PPE) in the air. At the excitation lower than 10.0 μJ, the microslice exhibits

weak-intensity emission and broad-spectrum representing spontaneous emission behavior. As PPE reaches 15 μJ, the emission intensity increases dramatically. At 15 μJ a PL sharp peak containing multiple spikes at around 600 nm appears. After background subtraction, the smallest full width at half-maximum (FWHM) of the spike is 0.2 nm provides evidence of coherent resonant feedback within the sample [23]. The small linewidth indicates a quality (Q) factor of 3000. Along with the rising in PL intensity, the overall PL linewidth becomes narrower as the PPE increase [24]. In more detail, Figure 3b shows the FWHM of PL emission from the microslice as a function of PPE. The spectral linewidth maintains at around 41.6 nm with excitation energy lower than 8.0 μJ then significantly reduces to 10.8 nm at 12 μJ. Finally, the spectral linewidth down to 4.2 nm at 15 μJ and nearly unchanged with higher PPE. Overall, the PL linewidth reduces nearly 10 times, from the initial value of 41.6 to 4.2 nm which is one of the key features of random lasing action.

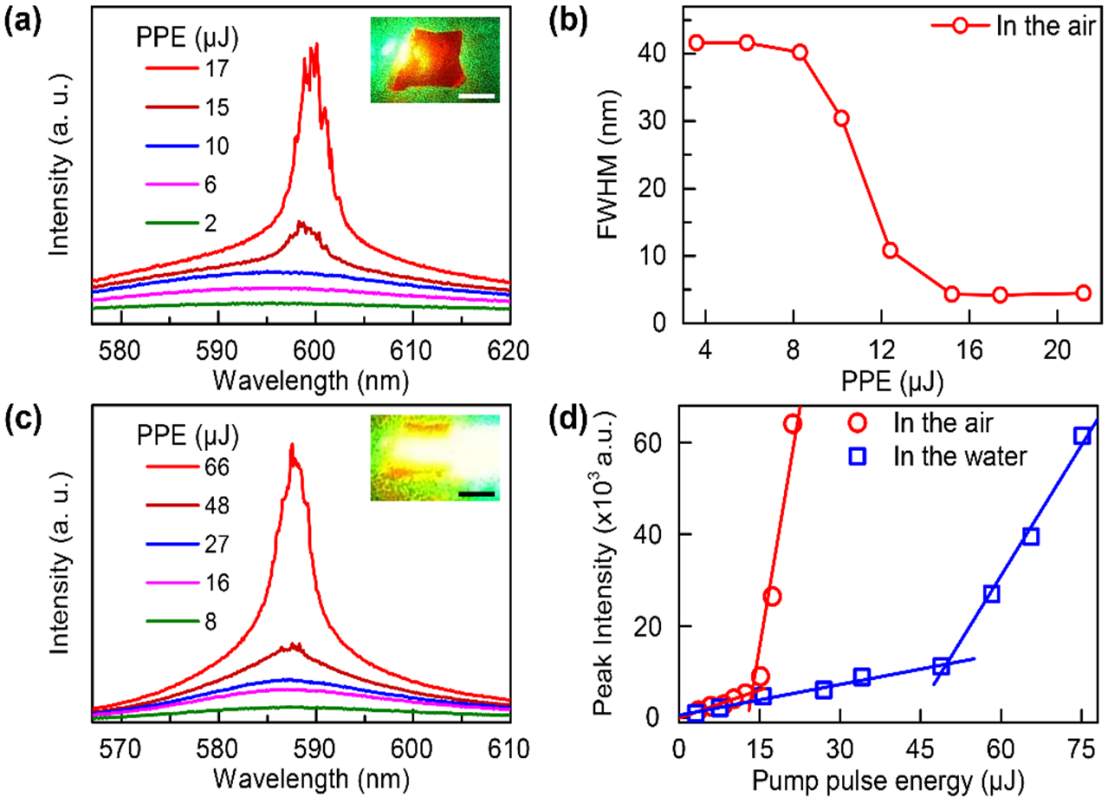

Fig. 3. (a) PL spectra from a single RhB-doped SNP microslice in the air. The inset shows the PL microscope image of the studied sample with a scale bar of 100 μm. (b) The corresponding PL linewith as a function of PPE. (c) PL spectra of the same microslice in the water. The inset shows the PL microscope image of the sample with a scale bar of 100 μm. (d) The peak intensity of the RhB-doped SNP microslice in the air and water as a function of pump pulse energy.

In the water, the sample exhibits a similar PL evolution but under a higher PPE (Fig. 3c). The emission starts narrowing at 48 μJ and the PL linewidth is down to 4.6 nm at 70 μJ. Only one spike with a spectral linewidth of 0.3 nm was observed thus Q-factor is $\sim$1950. As a result, the RhB-doped SNP microslices can work as random lasers in the air and water with a lasing threshold of less than 17 μJ (66 μJ) for the sample in the air (water). In addition, the lasing peak wavelength in the water is around 588 nm which is blue-shifted comparing with the lasing peak of 600 nm in the air. The reason for the shift will be discussed later.

Lasing threshold is one of the most significant behaviors of a laser [24]. The lasing threshold is indicated by a non-linear dependence of peak intensity on PPE. As shown in Fig. 3d, the PL intensity of the sample in the air (red circle) increases linearly with PPE until 15.0 μJ. Indeed, the PL intensity rises by a factor of 1.7 (from 2500 a. u. to 4150 a. u.) as the PPE increases from 6.0 to 10.0 μJ (also a factor of 1.7). However, a sudden rise in PL intensity is observed when the PPE reaches 15.0 μJ, the peak intensity is doubled to 9000 a. u. which indicates the evidence of a lasing threshold. Moreover, the intensity sharply rises from 9000 a. u. to 26000 a. u., nearly triples, when the PPE increases only a little from 15 to 17 μJ. The lasing threshold is determined to be about 14.2 μJ (the non-linear point) which is comparable with that of all-marine based random lasers [4] and cellulose-based random lasers [16]. A similar trend is also observed for the same sample immersed in the water but the lasing threshold (48.9 μJ) is 3 times higher than that in the air. Compared with other works, the threshold of the sample in the water is higher than that of the gold nanoparticles based random lasers [3] and silk based random lasers [7] which have been utilized for sensing in an aqueous medium.

III.2. Size-dependent lasing characteristics in the air and water

Size-dependent lasing threshold is an important character of a random laser but has been rarely investigated. In previous work, Ling *et al.* has addressed this issue indirectly by studying a relationship between the lasing threshold and the pump spot area [25]. Recently, Ta *et al.* showed a direct relationship between the lasing threshold (I_{th}) of microfiber random lasers with their size [26]. Generally, lasing threshold decreases with increasing their surface area. It is reasonable as a larger sample has a larger number of dye molecules thus more light is generated and amplified, leading to easier lasing action. However, there is no exact mathematical expression of the dependence between I_{th} and the pump spot area or sample surface area (A). Several works have shown that $I_{th} \sim A^{-\alpha}$, where α can ranges from 0.26 to 0.65 depending on a specific structure [26, 27]. In this work, we have found $I_{th} \sim A^{-0.66}$ for sample in the air and $I_{th} \sim A^{-0.45}$ for sample in the water (Fig. 4). Particularly, the smaller the laser size the higher the influence on lasing threshold. For samples with $A < 40\times10^3$ μm^2, I_{th} of the sample in the air decreases about 4.5 times (from 30 to 6.5 μJ) when the surface area increases by a factor of 7.5 (from 5×10^3 to 38×10^3 μm^2). Similar behaviour is also observed for the sample in the water. I_{th} reduces about 2 times (from 70 to 36 μJ) when the sample area increases 4 times (from 10×10^3 to 40×10^3 μm^2). In both cases, when $A > 40\times10^3$ μm^2, the lasing threshold is less influenced by the laser size.

In addition, the lasing threshold of samples in the water is higher than that of samples in the air. This result is understandable because the refractive index contrast of the sample in the water is lower thus the optical confinement is weaker compared with the sample in the air [7, 28]. Therefore, the light in the sample in the water is more likely to be scattered out which results in a higher optical loss and consequently a higher threshold. The difference can be as low as 3.5 times

for a sample with $A \sim 10\times10^3$ μm^2 and as high as 8 times for a sample with $A \sim 168\times10^3$ μm^2. The finding indicates that not only structure but also the working environment has a significant effect on the lasing performance and this information is important for the future use of silica-based random lasers in biosensing applications.

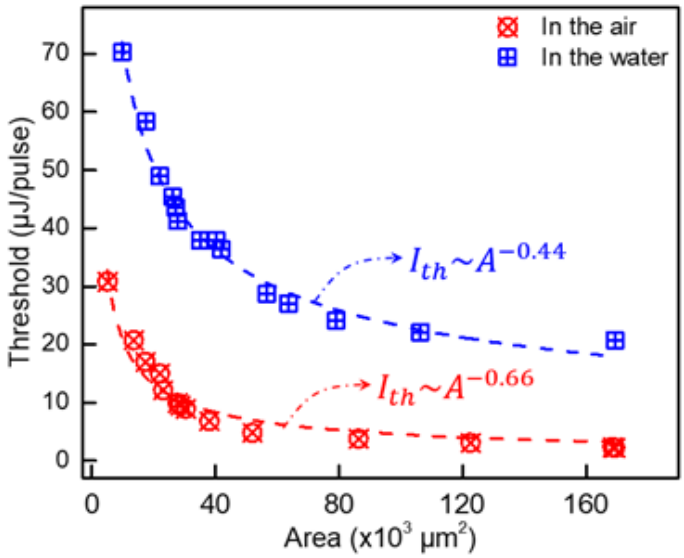

Fig. 4. Lasing threshold of silica-based random lasers (in the air and water) as a function of their surface area.

Not only the lasing threshold but the lasing wavelength is also affected the working environment. Due to the lower optical confinement, the lasing spectrum in the water is blue-shifted compared with the sample in the air. This phenomenon is common and frequently observed in microlasers [29]. As shown in Fig. 5a, a noticeable blue-shift of 12 nm is recorded for the sample with a surface area of 22×10^3 μm^2 when working in the air and water. For further investigation, the peak wavelength as a function of their surface area in both media is shown in Fig. 5b. Two distinct emitting regions can be observed. The average peak wavelength (λ_{aver}) of the samples with different surface areas (ranging from 10×10^3 to 168×10^3 μm^2) in the water is 586.8 nm which is 13.2 nm blue-shifted comparing with λ_{aver} (600.0 nm) of the samples in the air (surface areas ranges between 4×10^3 to 169×10^3 μm^2).

Furthermore, the linear fit dashed blue and red lines in Fig. 5b indicate that lasing peak moves to a longer wavelength as their size increases. This behavior is ascribed to the reabsorption of light of the dye molecules [26]. Indeed, as shown in Fig. 6a, emission from around 550 to 600 nm will be reabsorbed due to the overlap between absorption and fluorescence. Since the shorter wavelengths will be absorbed more than longer wavelengths thus the lasing emission is red-shifted. In addition, the longer the light travels, the higher chance it will be reabsorbed. Generally, as demonstrated in Figs. 6b and 6c, the emission light in a large sample travels a longer path compared with that in a small sample thus it is more likely to be reabsorbed. As a result, the lasing emission is red-shifted with increasing size.

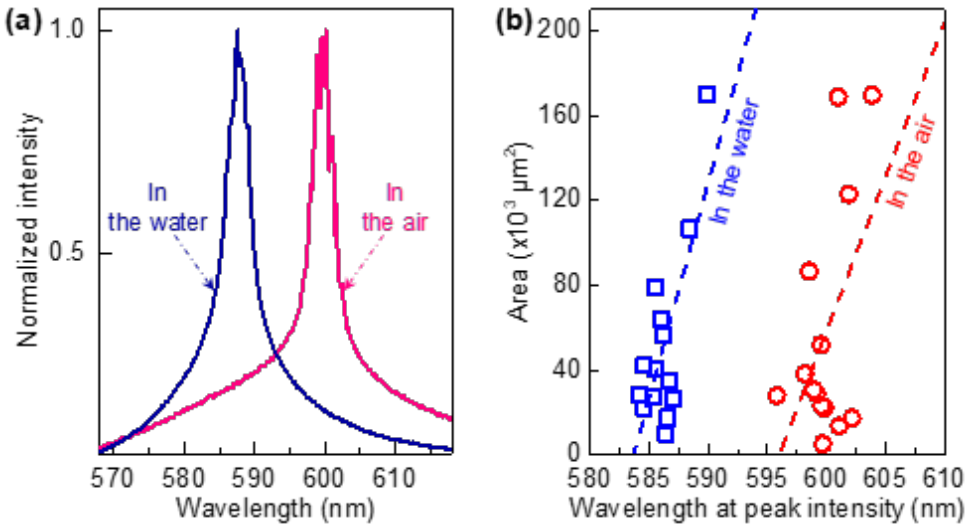

Fig. 5. (a) Normalized lasing spectrum of a typical RhB-doped SNP microslice in the air and the water. (b) The lasing peak wavelength of samples in the air (red circles) and the water (blue squares). (c) The absorption and fluorescence spectra of the RhB-doped SNPs.

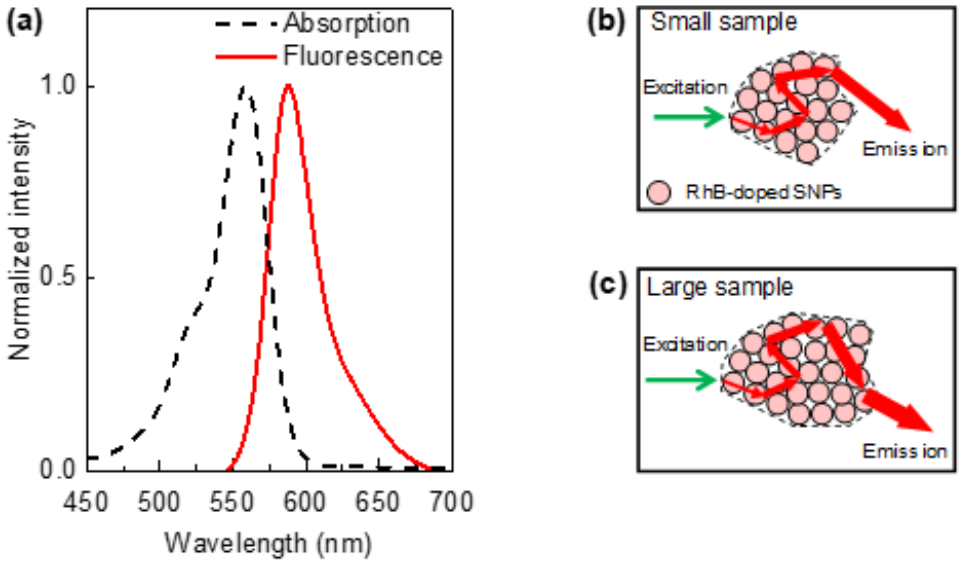

Fig. 6. (a) Absorption and fluorescence spectra of the RhB-doped SNPs. (b) and (c) Schematics demonstrate the light amplification via multiple scattering within a small and a larger sample, respectively.

IV. CONCLUSIONS

We have demonstrated that the laser size and working environment have significant effects on lasing characteristics of random lasers. The lasing threshold I_{th}decreases with increasing sample size such as $I_{\text{th}} \sim A^{-0.66}$ for sample in the air and $I_{\text{th}} \sim A^{-0.45}$ for sample in the water. For a similar size, the lasing threshold of the sample in the water is about 3-8 times (depending on the size) higher than that of the sample in the air. For the lasing wavelengths, it is red-shifted with increasing laser size. Herein, a shift of 8 nm of lasing peak wavelengths was recorded when the sample surface area increases from 21×10^3 to 169×10^3 μm^2. In addition, for a similar size, the lasing wavelengths of the sample in the water are blue-shift (13 nm on average) compared with that of the sample in the air. Our results have provided meaningful information for the future application of dye-doped SNP-based random lasers in bioimaging and biosensing.

ACKNOWLEDGMENTS

This work was funded by Le Quy Don Technical University under grant number 20.1.001

REFERENCES

[1] H. E. Türeci, L. Ge, S. Rotter, A. D. Stone, *Strong interactions in multimode random lasers*, *Science* **320** (2008) 643.

[2] Y. Wang, Z. Duan, Z. Qui, P. Zhang, J. Wu, A. Dingke and T. Xiang, *Random lasing in human tissues embedded with organic dyes for cancer diagnosis*, *Sci. Rep.* **7** (2017) 8385.

[3] W. Z. W. Ismail, G. Liu, K. Zhang, E. M. Goldys and J. M. Dawes, *Dopamine sensing and measurement using threshold and spectral measurements in random lasers*, *Opt. Express* **24** (2016) A85.

[4] B. Redding, M. A. Choma, H. Cao, Hui, *Dopamine sensing and measurement using threshold and spectral measurements in random lasers*, *Nat. Photonics* **6** (2012) 355.

[5] Q. Song, S. Xiao, Z. Xu, J. Liu, X. Sun, V. Drachev, V. M. Shalaev, O. Akkus, and Y. L. Kim, *Random lasing in bone tissue*, *Opt. Lett.* **35** (2010) 1425.

[6] R. C. Polson and Z. V. Vardeny, *Random lasing in human tissues*, *Appl. Phys. Lett.* **85** (2004) 1289.

[7] S. Caixeiro, M. Gaio, B. Marelli, F. G. Omenetto and R. Sapienza, *Silk-based biocompatible random lasing*, *Adv. Opt. Mater* **4** (2016) 998.

[8] V. W. Chen, N. Sobeshchuk, C. Lafargue, E. S. Mansfield, J. Yom, L. R. Johnstone, J. M. Hales, S. Bittner, S. Charpignon, D. Ulbricht, J. Lautru, I. Denisyuk, J. Zyss, J. W. Perry and M. Lebental, *Three-dimensional organic microlasers with low lasing thresholds fabricated by multiphoton and UV lithography*, *Opt. Express* **22** (2014) 12316.

[9] T. B. Messaoud, D. Wright, E. Toussaere, S. X. Dou and J. Zyss, *Laser threshold of polymer cylindrical microresonators*, *Synth. Met.* **138** (2003) 347

[10] H. Cao, Y. G. Zhao, S. T. Ho, E. W. Seelig, Q. H.Wang, R. P. H. Chang, *Random laser action in semiconductor powder*, *Phys. Rev. Lett.* **82** (1999) 2278

[11] Z. Shang, M. Yang and L. Deng, *Low–threshold and high intensity random lasing enhanced by $MnCl_2$*, *Materials* **9** (2016) 725

[12] P. Liu, S. Singh, Y. Guo, J. J. Wang, H. Xu, C. Silien, N. Liu and K. M. Ryan, *Assembling ordered nanorod superstructures and their application as microcavity lasers*, *Sci. Rep.* **7** (2017) 43884

[13] S. W. Chang, W. C. Liao, Y. M. Liao, H. I. Lin, H. Y. Lin, W. J. Lin, S. Y. Lin, P. Perumal, G. Haider, C. T. Tai, K. C. Shen, C. H. Chang, Y. F. Huang, T. Y. Lin and Y. F. Chen, *A white random laser*, *Sci. Rep.* **8** (2018) 2720

[14] F. Lahoz, I. R. Martín, M. Urgellés, J. Marrero-Alonso, R. Marín, C. J. Saavedra, A. Boto and M. Díaz, *Random laser in biological tissues impregnated with a fluorescent anticancer drug*, *Laser Phys. Lett.* **12** (2015) 045805

[15] C. S.Wang, T. Y. Chang, T. Y. Lin and Y. F. Chen, *Biologically inspired flexible quasi-single-mode random laser: An integration of Pieris canidia butterfly wing and semiconductors*, *Sci. Rep.* **4** (2014) 6736.

[16] M. V. Dos Santos, C. T. Dominguez, J. V. Schiavon, H. S. Barud, L. S. A. De Melo, S. J. L. Ribeiro, A. S. L. Gomes and C. B. De Araújo, *Random laser action from flexible biocellulose-based device*, *J. Appl. Phys.* **115** (2014) 083108

[17] H. N. Tran, T. H. L. Nghiem, T. T. Duong Vu, M. T. Pham, T. Van Nguyen, T. T. Tran, V. H. Chu, K. T. Tong, T. T. Tran, T. T. Xuan Le, J. C. Brochon, T. Q. Nguyen, M. N. Hoang, C. N. Duong, T. T. Nguyen, A. T. Hoang and P. H. Nguyen, *Dye-doped silica-based nanoparticles for bioapplications*, *Adv. Nat. Sci. Nanosci. Nanotechnol.* **4** (2013) 043001

[18] S. García-Revilla, J. Fernández, M. A. Illarramendi, B. García-Ramiro, R. Balda, H. Cui, M. Zayat and D. Levy, *Ultrafast random laser emission in a dye-doped silica gel powder*, *Opt. Express* **16** (2008) 12251

[19] B. García-Ramiro, M. A. Illarramendi, S. García-Revilla, R. Balda, D. Levy, M. Zayat and J. Fernández, *Lasing threshold of one- and two-photon-pumped dye-doped silica powder*, *Appl. Phys. B Lasers Opt.* **117** (2014) 1135

[20] V. D. Ta, T. T. Nguyen, T. H. L. Nghiem, H. N. Tran, A. T. Le, N. T. Dao, P. D. Duong and H. H. Mai, *Silica based biocompatible random lasers implantable in the skin*, *Opt. Commun.* **475** (2020) 126207

[21] R. D. Deegan, O. Bakajin, T. F. Dupont, G. Huber, S. R. Nagel and T. A. Witten, *Capillary flow as the cause of ring stains from dried liquid drops*, *Nature* **389** (1997) 827

[22] T. V. Nguyen, T. D. Nguyen, N. V. Pham, T.-A. Nguyen and D. V. Ta, *Characteristics of Dye-doped Silica Nanoparticles- Based Random Lasers in the Air and Water*, *Opt. Lett.* **46** (2021) 2517

[23] Y. Bian, X. Shi, M. Hu and Z. Wang, *A ring-shaped random laser in momentum space*, *Nanoscale* **12** (2020) 3166

[24] R. Sapienza, *Determining random lasing action*, *Nat. Rev. Phys.* **1** (2019) 690

[25] Y. Ling, H. Cao, A. L. Burin, M. A. Ratner, X. Liu and R. P. H. Chang, *Investigation of random lasers with resonant feedback*, *Phys. Rev. A - At. Mol. Opt. Phys.* **64** (2001) 8

[26] V. D. Ta, D. Saxena, S. Caixeiro and R. Sapienza, *Flexible and tensile microporous polymer fibers for wavelength-tunable random lasing*, *Nanoscale* **12** (2020) 12357

[27] Y. Chen, J. Herrnsdorf, B. Guilhabert, Y. Zhang, A. L. Kanibolotsky, P. J. Skabara, E. Gu, N. Laurand and M. D. Dawson, *Modification of emission wavelength in organic random lasers based on photonic glass*, *Org. Electron.* **13** (2012) 1129

[28] S. K. Y. Tang, R. Derda, Q. Quan, M. Lončar and G. M. Whitesides, *Continuously tunable microdroplet-laser in a microfluidic channel*, *Opt. Express* **19** (2011) 2204

[29] H. H. Mai, T. T. Nguyen, K. M. Giang, X. T. Do, T. Nguyen, H. C. Hoang and D. V. Ta, *Chicken albumen-based whispering gallery mode microlasers*, *Soft Matter* **16** (2020) 9069